

Cover Page



Universiteit Leiden



The handle <http://hdl.handle.net/1887/21936> holds various files of this Leiden University dissertation.

Author: Berg, Yascha Wilfred van den
Title: Tissue factor isoforms and cancer
Issue Date: 2013-10-08

Chapter 5 - Non-Proteolytic Properties of Murine Alternatively Spliced Tissue Factor: Implications for Integrin-Mediated Signaling in Murine Models

RC Godby*, YW van den Berg*, R Srinivasan, R Sturm, DY Hui, SF Konieczny, BJ Aronow, E Ozhegov, W Ruf, HH Versteeg*, and VY Bogdanov*

Mol Med. 2012 Jul 18;18:771-9.

(* denotes equal contribution)

Abstract

This study was performed to ascertain whether murine alternatively spliced Tissue Factor (masTF) acts analogously to human asTF (hasTF) in promoting neovascularization via integrin ligation. Immunohistochemical evaluation of a spontaneous murine pancreatic ductal adenocarcinoma (PDAC) model revealed increased levels of masTF and murine full-length TF (mflTF) in tumor lesions compared to benign pancreas; furthermore, masTF co-localized with mflTF in spontaneous aortic plaques of *Ldlr*^{-/-} mice, indicating that masTF is likely involved in atherogenesis and tumorigenesis. Recombinant masTF was used to perform *in vitro* and *ex vivo* studies examining its integrin-mediated biologic activity. Murine endothelial cells (EC) rapidly adhered to masTF in a β 3-dependent fashion. Using adult and embryonic murine EC, masTF potentiated cell migration in transwell assays. Scratch assays were performed using murine and primary human EC; the effects of masTF and hasTF were comparable in murine EC, but in human EC the effects of hasTF were more pronounced. In aortic sprouting assays, the potency of masTF-triggered vessel growth was undistinguishable from that observed with hasTF. The pro-angiogenic effects of masTF were found to be *Ccl2*-mediated, yet independent of VEGF. In murine EC, masTF and hasTF upregulated genes involved in inflammatory responses; murine and human EC stimulated with masTF and hasTF exhibited increased interaction with murine monocytic cells under orbital shear. We propose that masTF is a functional homolog of hasTF, exerting some of its key effects via β 3 integrins. Our findings have implications for the development of murine models to examine the interplay between blood coagulation, atherosclerosis, and cancer.

Introduction

Tissue Factor (TF), an integral membrane glycoprotein, serves as an enzymatic co-factor of the serine protease FVII/FVIIa and acts as the principle physiologic trigger of the blood coagulation cascade. Aside from its role in the maintenance of normal hemostasis and its involvement in a variety of thrombotic disorders, TF is known to affect angiogenesis via protease activated receptor-2 (PAR-2) signaling and interactions with α 3 β 1 and α 6 β 1 integrins¹.

The term angiogenesis collectively refers to the processes that result in the formation of new vasculature from pre-existing blood vessels. Angiogenesis depends on a delicate interplay between the endothelium and pericytes^{2,3}. Initially, tip cells migrate from the existing vessel and are followed by stalk cells, which divide and form a lumen, thus creating a capillary⁴. The tip cell also mediates recruitment of pericytes which then align the capillary⁵. This process is carefully regulated by key angiogenic molecules such as

vascular endothelial growth factor (VEGF), platelet derived growth factor (PDGF), various metalloproteinases, and interleukin-8 (IL-8)⁶⁻⁸. However, angiogenesis is also critically dependent on integrin function. Integrins are heterodimeric receptors that are formed by the combination of 18 possible α -subunits and 8 β -subunits to form 20 separate extracellular matrix-binding receptors⁹. These receptors, specifically β 1 and β 3-type integrins, play a critical role in endothelial cell and pericyte migration, but are also indispensable in the formation of capillaries^{10,11}. Although beneficial in certain physiologic settings e.g., embryonic development and wound healing, neovascularization is the sine qua non of primary tumor growth and metastasis, and in atherosclerosis, vasa vasorum is thought to be the major contributor to plaque instability¹².

Within the past decade, a soluble, naturally occurring TF splice variant (asTF) lacking a transmembrane domain was discovered¹³. Absence of exon 5 in asTF's mRNA results in an open reading frame shift, giving rise to a unique C-terminus. asTF can be secreted, exhibits minimal coagulant potential compared to the membrane-bound full-length TF (flTF) and is detectable, alongside flTF, in spontaneously formed arterial thrombi. Discernible pro-coagulant activity of native asTF was demonstrated to be low and phospholipid-dependent¹⁴; biosynthesis of asTF in monocytes and endothelial cells is controlled by several splicing regulator (SR) proteins, most notably ASF/SF2 and SRp55, and a group of kinases comprising Cdc2-like kinase, DNA topoisomerase I, and phosphatidylinositol-3 kinase¹⁵⁻¹⁷. Following the discovery of human asTF (hasTF), its murine homolog (masTF) was identified and characterized¹⁸. Like hasTF, masTF lacks a transmembrane domain due to the exclusion of exon 5 from the primary transcript during pre-mRNA splicing, and has a distinct 93-amino acid C-terminus, rendering it soluble. While masTF was detected in abundance in organized arterial thrombi, as well as FeCl₃-induced acute thrombi in mice systemically challenged with lipopolysaccharide (LPS)^{18,19}, masTF's functional contribution to any of the disease states that have been modeled *in vivo* – e.g. tumorigenesis and atherothrombosis – has yet to be established²⁰.

We recently reported that hasTF induces angiogenesis and promotes monocyte-endothelial interactions via integrin ligation, without engagement of protease activity^{21,22}. Thus, hasTF may be of interest in the field of anti-cancer therapies targeting neovascularization. Intriguingly, it was recently reported that overexpression of masTF in murine cardiomyocytes elicited increased production of pro-migratory and pro-angiogenic factors by these cells, although the molecular mechanisms underlying these effects of masTF were not fully ascertained²³. Because murine models comprise the preferred *in vivo* platform for cancer and cardiovascular research, it is imperative to determine whether

masTF is a functional homolog of hasTF, especially with regard to non-proteolytic, integrin-mediated events promoting vessel growth.

We here report, for the first time, that masTF possesses integrin-mediated biologic properties highly analogous to those of hasTF, indicating that secreted variants of mammalian TF may generally act as agonists promoting neovascularization and monocyte recruitment via integrin ligation.

Materials and Methods

Reagents/antibodies- Murine TF isoform-specific polyclonal antibodies were described previously¹². In vitro angiogenesis kit (Matrigel) was obtained from Millipore (Billerica, MA). Anti-mouse β 1 (9EG7) and β 3 (2C9.G2) antibodies were from BD Pharmingen (Franklin Lakes, NJ). Recombinant mouse VEGF was purchased from Invitrogen (Carlsbad, CA). Transwell permeable supports with 8 μ m pore size were from Costar (Corning, NY). Isolectin B4 was from Vector Laboratories (Burlingame, CA). Calcein-AM was from BD Biosciences (San Jose, CA). Anti-murine p65/RelA polyclonal antibody was from Santa Cruz Biotechnology (Santa Cruz, CA). SU5416 was from EMD Biosciences (San Diego, CA). Rabbit anti-mouse Ccl-2 antibody was from Acris Antibodies GmbH (Herford, Germany). Recombinant ectodomain of murine flTF was produced and characterized as described²⁴.

Immunohistochemistry- The K-ras induced pancreatic ductal adenocarcinoma (PDAC) murine model and atherosclerosis-prone Ldlr^{-/-} mice were described previously^{25,26}. Serial sections of formalin fixed, paraffin embedded specimens were deparaffinized and rehydrated, endogenous peroxidase was blocked, and expression of masTF and mflTF was assessed using standard immunohistochemical techniques²². Sections of murine atherosclerotic lesions were also assessed for masTF and mflTF co-localization with monocytes/macrophages by staining with anti-CD68 antibody (Santa Cruz).

Generation of recombinant asTF proteins- N-terminally His-tagged recombinant hasTF was generated, purified, and characterized as previously described²². N-terminally His-tagged recombinant masTF mature protein was generated in E. Coli, purified, and assessed by Coomassie staining; masTF's identity was confirmed by western blotting (not shown).

Cell culture- Murine EC (bEnd.3 from the ATCC and MEEC, provided by Dr M.J. Goumans, LUMC), primary human retinal endothelial cells (HREC, Cell Systems) and murine monocytes/macrophages (J774A.1, ATCC) were grown in filter-cap tissue culture flasks containing DMEM media supplemented with 10% Fetal Bovine Serum (FBS) and penicillin/streptomycin (all from Hyclone/Thermo Scientific, Rockford, IL). Incubators were

maintained at 37°C and 5% CO₂. T75 Cell culture flasks and other cell culture disposables were purchased from Greiner Bio-One (Alphen a/d Rijn, the Netherlands).

EC adhesion assay- 96 well plates were coated with 50 µL of 50 nM masTF and 50 µL 10% BSA overnight. 2X10⁴ bEnd.3 cells were added in 100 µL serum-free DMEM to each well for both conditions, and the plates then were placed in a 5% CO₂ incubator at 37°C for four hours. The wells were washed with PBS, and the adherent cells fixed in methanol and stained with 0.1% Crystal Violet. In some experiments, 96 wells plates were coated with 50 µL masTF at a concentration of 50 µg/mL, 10% BSA (negative control), or 1% gelatin (positive control) for one hour at 37°C; subsequently, blocking was performed under the same conditions with 10% BSA. Then, 2X10⁴ bEnd.3 cells were seeded per well after 20 minutes incubation with integrin-blocking antibodies depending on the conditions at a concentration of 50 µg/mL. After five hours, images were captured using a camera equipped microscope and flattened cells per view field were counted.

EC migration assay- The lower sides of 8 µm pore transwell inserts were coated with 50 µL masTF at a concentration of 50 µg/mL for one hour at 37°C, 10% BSA (negative control) or 1% gelatin (positive control). bEnd.3 cells or murine embryonic endothelial cells (MEEC) were trypsinized, and incubated with integrin-blocking antibodies for 20 minutes at a concentration of 50 µg/mL when appropriate. 2X10⁴ cells were seeded per well in DMEM containing 10% FBS and left to migrate overnight. Filters were fixed in 4% phosphate-buffered formaldehyde, stained with crystal violet, and washed in PBS; hereafter cells on the top side of the filter were removed with a cotton swab. Microscope pictures were taken from the middle of the inserts and cells were counted per magnification field. All experiments are performed in triplicates.

Scratch assay- bEnd.3 cells and HREC were grown to confluence in six well plates and maintained overnight in DMEM media containing 2% FBS. Subsequently, 8 radial scratches per well were introduced using a 20 µL pipette tip. Cells were treated with masTF, hasTF, VEGF, or PBS and glycerol (vehicle control) in 1 mL of DMEM containing 10% FBS and incubated at 37°C, 5%CO₂. After 38 hours, the cells were rinsed with PBS, fixed in methanol, and stained with 0.1% Crystal Violet. The plates were placed on the platform of an inverted microscope, pictures of a single radial wound (8 pictures per well) were captured at low magnification using a digital camera (SD1200IS, Canon). Analyses were carried out using Image J software - pictures were converted to binary, the area of the cells was measured, and each wound area was then measured relative to the area of the cells. The area of the cells was used to normalize the area of the wound. Final pixilation of each scratch was converted to mm².

Aortic sprouting assay- Male C57Bl/6 mice were obtained from Harlan Sprague-Dawley, Horst, The Netherlands and were maintained at the animal care facility of the Leiden University Medical Center according to the institutional guidelines. Animal procedures were carried out in compliance with Institutional Standards for Humane Care and Use of Laboratory Animals. The Animal Care and Use Committee of the Leiden University Center approved all experiments. Mice ranging in age from 9-11 weeks were sacrificed by cervical dislocation. Aortas were dissected, cleaned and flushed with serum free RPMI. Subsequently, aortas were cut into ~1 mm segments, embedded into 70 μ L Matrigel, and left in a 37°C incubator to polymerize. Matrigel was supplemented with either masTF, hasTF, 5 μ M SU5416 (VEGFR2 inhibitor), anti-Ccl2 antibody (final concentration 10.0 μ g/mL), or buffer control depending on the experimental conditions. A 9:1 medium mixture of M199:EGM and 100 μ g/mL streptomycin and 100 units/mL penicillin was used to cover the embedded aortic segments. Integrin blockade was performed by addition of antibodies to the Matrigel at a concentration of 50 μ g/mL, when appropriate.

Microarray Analysis- bEnd.3 cells were grown to confluence in six-well plates and treated with 50 nM masTF (excluding controls) for six hours; total RNA was extracted using Qiagen RNeasy Mini Kit (Valencia, CA), reverse transcribed, amplified, fragmented, and labeled for microarray analysis using the Nugen WT-Ovation FFPE V2 kit, Exon Module, and Encore biotin module, respectively (Nugen) according to the manufacturer's instructions. An Affymetrix Gene 1.0 ST microarray platform was used to assess the gene expression profile (Microarray Core Facility, Cincinnati Children's Hospital and Medical Center). Gene transcripts were identified based on filtering for probesets with Robust Multichip Average-normalized raw expression of greater than 6.0, that differed between treated with either masTF or hasTF and untreated EC by at least 1.2 fold for upregulated genes and at least 0.9 fold for downregulated genes with $p < 0.05$ using a Welch t-test. Using this approach, 338 probesets were identified that were differentially upregulated, of which 133 were up-regulated and 205 were down-regulated. Of these 338 probesets, 264 genes were protein-coding (listed in Supplementary Table 1).

Orbital shear assay- bEnd.3 cells and HREC were grown to confluence in 96 well plates and treated with masTF or hasTF for four hours. Subsequently, J774A.1 cells pre-labeled with Calcein-AM at 1 μ M final concentration, washed free of unlabeled dye, were added at 1×10^5 cells/well. The plates were placed on a horizontal orbital shaker and left rotating at 90 rpm in a 5% CO₂ incubator at 37°C for 20 minutes. Non-adherent J774A.1 cells were washed away with PBS, adherent cells lysed in PBS containing 0.5% Triton-X, and fluorescence was measured at Ex-485 and Em-515.

Results

Expression of masTF and mflTF in pancreatic cancer lesions and co-localization with CD68-positive cells in atherosclerotic plaques- Expression of hasTF has been detected in many PDAC cell lines, and hasTF was previously shown to promote tumor growth^{27,28}. We examined the expression patterns of masTF and mflTF in pancreatic tissue of genetically modified mice that spontaneously develop preneoplastic lesions (PanINs) and PDAC; as shown in Fig. 1A, the intensity of staining for masTF as well as mflTF increased as lesions progressed from early PanINs to high-grade PDAC phenotype, indicating that masTF is likely to contribute to pancreatic tumor growth in the murine setting. Compared to mflTF, staining for masTF in PanINs and PDAC tissue appeared to be somewhat more diffuse; to ascertain whether masTF is present in the extracellular stromal compartment, immunofluorescence studies were performed and as shown in Fig. 1B, masTF was found in abundance in tumor cells as well as extracellular stroma, whereas mflTF was exclusively cell-associated. K-ras-triggered upregulation of NF κ B is a well established pathological feature of PDAC (29), and transcription of human as well as murine TF-encoding genes (F3 and Cf3, respectively) is markedly responsive to NF κ B. Examination of murine pancreatic tissue for the levels of p65/RelA revealed that normal pancreas was negative, whereas PDAC tissue had high levels of p65/RelA with some tumor cells exhibiting pronounced nuclear redistribution of p65/RelA (Fig. 1C). Aside from neoplastic diseases, neovascularization plays a critical role in plaque remodeling¹². While we previously demonstrated that masTF is present in experimental occlusive thrombi in the wire injury model¹⁷ and hasTF was detected in aortic plaques^{22,30}, it is not known whether masTF is present in aortic plaques. Appreciable levels of masTF were detectable in Ldlr $^{-/-}$ plaques (Fig. 1D), where extensive co-localization of masTF with mflTF and CD68-positive cells was observed (Fig. 1E).

masTF and hasTF bind integrins on murine EC and elicit migration in a transwell assay- Since hasTF was previously shown to bind integrins, masTF may similarly influence cell behavior through integrin ligation. To study this, tissue culture plates were coated with masTF, mflTF or hasTF and blocked with BSA, after which bEnd.3 cells were seeded. bEnd.3 cells avidly bound to masTF, mflTF and hasTF-coated plates, but very poorly to BSA-coated plates (Fig. 2A). To identify the possible involvement of integrins, bEnd.3 cells were pre-incubated with specific blocking antibodies. Inclusion of a β 3 integrin-blocking antibody dramatically inhibited EC binding to masTF (Fig. 2B). We previously showed that EC binding to hasTF is inhibited by β 1 blockade. Nevertheless, binding of bEnd.3 cells to masTF was not disrupted by β 1 blockade, and the combination of β 1 and β 3 blockades showed a similar reduction of cell adhesion when compared to a selective β 3 blockade

(Fig. 2B). Thus, $\beta 3$ integrins – but not $\beta 1$ integrins – appear to predominate in masTF-murine EC interactions. As we previously showed that hasTF is a potent inducer of EC migration in a transwell migration assay, we sought to ascertain whether masTF protein exhibits similar properties. Indeed, a 5-fold upregulation of bEnd.3 cell migration was observed in transwells that were coated with masTF. To determine the identity of the involved integrins, we treated EC with integrin-blocking antibodies prior to the assay. As was observed before for hasTF, masTF-induced EC migration was shown to solely depend on $\beta 3$ integrins (Fig. 2C); analogous results were obtained when MEEC were used in this assay (Supplementary Fig. 1).

masTF and hasTF are potent agonists in a scratch assay- Scratch assays are often used to assess cellular motility, invasion, and intercellular interactions³¹. To determine if, aside from the gradient-type/transwell system, masTF and/or hasTF are able to potentiate scratch closure, we employed a scratch assay using bEnd.3 cells and HREC to assess the relative degree of potency. Per scratch, the enhancement of bEnd.3 closure by masTF (1 nM) was not distinguishable from that elicited by VEGF (2 nM, ~2 fold over vehicle control; $p < 0.01$, Fig. 3A). The effects of mlTF (1 nM) were similar to those of masTF, yet hasTF was less potent at 1 nM; at 10 nM, all three forms of TF exhibited similar potency (Fig. 3A). When HREC were employed in the scratch assay, hasTF was markedly more potent than masTF in the 1-10 nM range (Fig. 3B).

masTF induces vessel growth ex vivo- Since hasTF mediates angiogenesis and the biologic effects of masTF observed in vitro are in line with the in vitro effects of hasTF, we next assessed whether masTF promotes angiogenesis *ex vivo*. Using aortic sprouting assays, we were able to confirm that masTF induces the formation of new vessels with the levels of potency indistinguishable from that of hasTF in the 1-100 nM range (Fig. 5A). Next we determined whether masTF-induced *ex vivo* angiogenesis is integrin-dependent and we indeed observed sprouting comparable to basal levels in the presence of $\beta 3$ blocking antibodies; however, a $\beta 1$ blockade also resulted in a down regulation of *ex vivo* angiogenesis, in the absence as well as the presence of exogenously added masTF (Fig. 4A). As Matrigel consists primarily of $\beta 1$ integrin-ligating extracellular matrix proteins, it is plausible that the synergy between $\beta 1$ -ligating matrigel and $\beta 3$ -ligating masTF is required for the masTF-dependent formation of sprouts and as such, masTF possesses angiogenic properties analogous to those of hasTF. Strikingly, antibody blockade of Ccl2 – a chemokine recently shown to be critical for flTF-mediated angiogenesis³² – completely eliminated the effect of masTF, indicating that Ccl2 is indispensable for masTF-mediated pro-angiogenic effects (Fig. 4A). However, VEGF blockade, while diminishing the basal angiogenesis, did not eliminate the pro-angiogenic effects of masTF in this assay (Fig. 4B).

We note that we detected low levels of endogenous masTF protein in our Matrigel cultures by Western blotting (data not shown). When mfITF ectodomain was added to the cultures, there appeared to be a weak increase in sprouting that did not reach statistical significance (Fig. 4B).

masTF and hasTF elicit analogous changes in the global expression profile of murine EC- While the signaling events elicited by hasTF in human EC were investigated previously²², nothing is known about the changes in gene expression in murine EC elicited by masTF. bEnd.3 cells stimulated with masTF and hasTF revealed significant nuclear redistribution of p65/Rel A (Fig. 5A). Microarray analysis revealed that hasTF and masTF exert similar effects on global gene expression in murine EC (Fig 5B). A significant number of genes were upregulated as well as downregulated by both masTF and hasTF; the list of these genes is presented in Supplementary Table 1. The major genes that were significantly upregulated were chemokine family genes, such as Cxcl2, Csf-1, and Ccl2. Integrin linked kinase (ILK) is a binding partner for β 1 and β 3 integrins, and helps in anchoring β 1 and β 3 integrins to the actin cytoskeleton. ILK-mediated signaling has been shown to significantly upregulate SDF1 (Cxcl12) expression in human EC³³. Since we established that hasTF, and now masTF, ligate integrins, it could well trigger ILK-dependent signaling in murine EC. Analogously to human microvascular EC, whose exposure to hasTF resulted in the upregulation of NFkB pathway-related chemokines²², hasTF and masTF elicited activation of NFkB dependent pathways in murine EC (Fig. 5B).

masTF and hasTF promote monocyte adhesion to murine EC- While the expression of cell adhesion molecules on murine EC was not upregulated as dramatically in response to masTF and/or hasTF as was shown for human ECs²², Vcam-1 – the gene encoding an adhesion molecule critical to EC-monocyte interactions – was upregulated by ~6.5 fold in response to both masTF and hasTF (Supplementary Table 1, Fig. 6A), which is significant since even a modest increase in the levels of VCAM-1 reflects a state of activated endothelium³⁴. Having established that masTF, like hasTF, is present in aortic plaques and induces the expression of chemokines in murine EC (Figs 1, 5), we sought to determine whether masTF promotes adhesion of murine monocytes to murine and/or human EC. As shown in Figure 6B,C, masTF as well as hasTF elicited a significant increase in the adhesion of murine monocytes to bEnd.3 cells and HREC under orbital shear conditions.

Discussion

The major novel findings we report here are as follows: I. masTF is biologically active; II. the biologic effects of masTF are analogous to those of hasTF, and can be experimentally assessed using murine as well as human cell cultures; III. masTF-mediated angiogenesis is

dependent on $\beta 1$ and $\beta 3$ integrins as well as Ccl-2, yet independent of VEGF. Specifically, we show for the first time that the murine form of asTF is a functional homolog of hasTF inasmuch as it acts as an agonist on EC surfaces in promoting cell adhesion, migration, and neovascularization in an integrin-mediated fashion. While the importance of the TF-integrin axis has been known for some time, it has been shown that the flTF-integrin crosstalk primarily involves $\beta 1$, not $\beta 3$ integrins¹; thus, $\beta 3$ -mediated events may very well be uniquely regulated by asTF in human as well as murine solid tissues. Strikingly, murine ECs do not appear to engage $\beta 1$ integrins while adhering to masTF (Fig. 2), yet both $\beta 1$ and $\beta 3$ integrins are required for masTF-elicited angiogenesis, analogously to the hasTF (Fig. 4)²¹. It should be noted that $\beta 3$ -deficient mice exhibit a pathological enhancement of angiogenesis rather than inhibition of vessel growth³⁵; however, aberrations triggered by global $\beta 3$ deficiency may not be reflective of the effects elicited by soluble $\beta 3$ ligands (e.g., masTF/hasTF) in select tissue sub-compartments (e.g., the vasculature). While it cannot be excluded that the relative abundance of $\beta 1$ vs. $\beta 3$ integrins may influence experimental outcomes in studies involving distinct EC lines/sub-types²², the differences in global gene expression changes elicited by hasTF in human ECs, and masTF in murine ECs are also likely to play a role. The divergence of the gene expression cascades notwithstanding, the end-results of masTF-murine EC interactions, i.e., angiogenesis and monocyte recruitment, are remarkably analogous to those of hasTF-human EC interactions. The structure of asTF's unique C-terminus is another aspect of asTF biology that may explain the differential "integrin profiles" of masTF and hasTF. masTF has a longer C-terminal domain compared to hasTF and may confer a distinct, masTF-unique conformation, resulting in the activation of a different subset of integrins. We note that in silico searches for potential integrin-binding sites within unique C-termini of hasTF and masTF did not yield any candidate motifs (Godby et al, unpublished data); thus, further studies on the functional role(s) of the hasTF and masTF C-termini and its physiological implications are warranted.

Our findings are in agreement with those of other groups that recently reported upregulation of such pro-angiogenic molecules as VEGF, basis fibroblast growth factor (bFGF), and Cyr61 as a result of masTF overexpression in murine cardiomyocytes^{23,36}; VEGF-independent nature of masTF-elicited effects in the sprouting assay and the gene array analysis suggest that murine EC may react to masTF in ways not fully identical to those observed in cardiac tissue (Fig. 4, 5). Cxcl2 – a gene analogous to Il-8 – encodes a major inflammatory chemokine involved in the recruitment of inflammatory cells^{37,38}, whereas Csf-1 production by stromal cells has been linked to the increased recruitment of Tumor-Associated Macrophages (TAM) and propagation of metastases³⁹. Genes encoding regulatory transcription factors were also upregulated in masTF and hasTF treated cells,

e.g. Cebpd. We note that Cebpd is involved in tumor suppression, and its increased expression might be due to a feedback response to the upregulation of inflammatory/tumor activating genes. Interestingly, the expression of Gja5 – the gene encoding a gap junction protein whose loss is associated with decreased endothelial relaxation and eNOS levels in the mouse aorta⁴⁰ – was downregulated by masTF and hasTF, raising the possibility that the effects of these soluble TF variants may exacerbate systemic vasculopathies related to aberrant eNOS activity.

While we are currently dissecting what signaling cascades are engaged by masTF in murine EC, the results of our study clearly demonstrate that there are many similarities between masTF and hasTF when it comes to their targets. It is worth noting that $\beta 3$ integrins play a comparably crucial role in cardiovascular disease and cancer – the conditions hallmarked by chronic inflammatory events, a common feature in the pathobiology of atherosclerosis and solid malignancies^{41,42}. As the levels of masTF rise in the course of pancreatic cancer progression (Fig. 1), it is worth noting that $\alpha v\beta 3$ – the integrin known to interact with hasTF – plays a particularly major role in pancreatic cancer pathobiology. The $\alpha v\beta 3$ dimer, a major RGD receptor, is perceived to exert its tumor-promoting effects through adhesion-mediated modulation of tumor cell invasiveness and proliferative/migratory capacity, as well as promoting metastatic neovascularization: compared to normal microvessels, metastatic microvessels express higher levels of this integrin⁴³. However, $\alpha v\beta 3$ is also expressed in PDAC cells and was reported to play a significant adhesion-independent role in pancreatic cancer⁴⁴. masTF appears to act as a cell agonist by ligating $\beta 3$ integrins on ECs, which activates the NF κ B pathway (Fig. 5A). The $\beta 3$ -asTF nexus may thus promote tumorigenesis directly via autocrine stimulation of cancer cells, as well as indirectly via neovascularization. The tenet that the flTF/asTF synergy promotes primary tumor growth and, possibly, spread is supported by the effects of mAb 10H10, a flTF-specific antibody that disrupts constitutive binding of flTF to integrins, and also inhibits tumor growth in xenograft models⁴⁵. Moreover, Ccl2-dependent nature of masTF-elicited angiogenesis further supports the notion that asTF and flTF are likely to act in concert to trigger the formation of new vessels, employing proteolytic as well as non-proteolytic signaling³². Inasmuch as exogenous flTF on microparticles and lipid vesicles stimulates cell proliferation largely in a $\beta 1$ integrin-dependent manner⁴⁶, it is reasonable to propose that asTF similarly promotes integrin-mediated tumorigenesis, yet with a far more pronounced engagement of $\beta 3$ integrins. Future experiments should reveal whether asTF acts as a pro-angiogenic as well as mitogenic agent *in vivo*.

Acknowledgements

This study was partially supported by NIH grant HL094891 to V.Y.B., NIH CA124586 to S.F.K., and by the Netherlands Organization for Scientific Research (NWO grant 17.106.329) to H.H.V.

References

1. Versteeg HH, Ruf W. (2006) Emerging insights in tissue factor-dependent signaling events. *Semin Thromb Hemost.* 32(1):24-32.
2. Armulik A, Abramsson A, Betsholtz C. (2005) Endothelial/pericyte interactions. *Circ Res.* 97(6):512-23.
3. Carmeliet P, Jain RK. (2011) Molecular mechanisms and clinical applications of angiogenesis. *Nature.* 473(7347):298-307.
4. Holderfield MT, Hughes CC. (2008) Crosstalk between vascular endothelial growth factor, notch, and transforming growth factor-beta in vascular morphogenesis. *Circ Res.* 102(6):637-52.
5. Gaengel K, Genové G, Armulik A, Betsholtz C. (2009) Endothelial-mural cell signaling in vascular development and angiogenesis. *Arterioscler Thromb Vasc Biol.* 29(5):630-8.
6. Ferrara N, Gerber HP, LeCouter J. (2003) The biology of VEGF and its receptors. *Nat Med.* 9(6):669-76.
7. Rundhaug JE. (2005) Matrix metalloproteinases and angiogenesis. *J Cell Mol Med.* 9(2):267-85.
8. Li A, Dubey S, Varney ML, Dave BJ, Singh RK. (2003) IL-8 directly enhanced endothelial cell survival, proliferation, and matrix metalloproteinases production and regulated angiogenesis. *J Immunol.* 170(6):3369-76.
9. Hynes RO. (2002) Integrins: bidirectional, allosteric signaling machines. *Cell.* 110(6):673-87.
10. Brooks PC, Clark RA, Chersesh DA. (1994) Requirement of vascular integrin alpha v beta 3 for angiogenesis. *Science.* 264(5158):569-71.
11. Bloch W, et al. (1997) Beta 1 integrin is essential for teratoma growth and angiogenesis. *J Cell Biol.* 139(1):265-78.
12. Galis ZS, Lessner SM. (2009) Will the real plaque vasculature please stand up? Why we need to distinguish the vasa plaquorum from the vasa vasorum. *Trends Cardiovasc Med.* 19(3):87-94.
13. Bogdanov VY, et al. (2003) Alternatively spliced human tissue factor: a circulating, soluble, thrombogenic protein. *Nat Med.* 9(4):458-62.
14. Szotowski B, Antoniak S, Poller W, Schultheiss HP, Rauch U. (2005) Procoagulant soluble tissue factor is released from endothelial cells in response to inflammatory cytokines. *Circ Res.* 96(12):1233-9.
15. Tardos JG, et al. (2008) SR proteins ASF/SF2 and SRp55 participate in tissue factor biosynthesis in human monocytic cells. *J Thromb Haemost.* 6(5):877-84.
16. Eisenreich A, et al. (2009) Cdc2-like kinases and DNA topoisomerase I regulate alternative splicing of tissue factor in human endothelial cells. *Circ Res.* 104(5):589-99.
17. Eisenreich A, et al. (2009) Role of the phosphatidylinositol 3-kinase/protein kinase B pathway in regulating alternative splicing of tissue factor mRNA in human endothelial cells. *Circ J.* 73(9):1746-52.
18. Bogdanov VY, et al. (2006) Identification and characterization of murine alternatively spliced tissue factor. *J Thromb Haemost.* 4(1):158-67.
19. Brüggemann LW, Drijfhout JW, Reitsma PH, Spek CA. (2006) Alternatively spliced tissue factor in mice: induction by *Streptococcus pneumoniae*. *J Thromb Haemost.* 4(4):918-20.
20. Srinivasan R, Bogdanov VY. (2011) Alternatively spliced tissue factor: discovery, insights, clinical implications. *Front Biosci.* 17:3061-71.

21. van den Berg YW, et al. (2009) Alternatively spliced tissue factor induces angiogenesis through integrin ligation. *Proc Natl Acad Sci U S A.* 106(46):19497-502.
22. Srinivasan R, et al. (2011) Splice Variants of Tissue Factor Promote Monocyte-Endothelial Interactions by Triggering the Expression of Cell Adhesion Molecules via Integrin-Mediated Signaling. *J Thromb Haemost.* 9(10):2087-96.
23. Eisenreich A, Boltzen U, Malz R, Schultheiss HP, Rauch U. (2011) Overexpression of alternatively spliced tissue factor induces the pro-angiogenic properties of murine cardiomyocytic HL-1 cells. *Circ J.* 75(5):1235-42.
24. Disse OJ, et al. (2011) The endothelial protein C receptor supports tissue factor ternary coagulation initiation complex signaling through protease-activated receptors. *J Biol.Chem.* 286 (7):5756-67.
25. Habbe N, et al. (2008) Spontaneous induction of murine pancreatic intraepithelial neoplasia (mPanIN) by acinar cell targeting of oncogenic Kras in adult mice. *Proc Natl Acad Sci U S A.* 105(48):18913-8.
26. Swertfeger DK, Bu G, Hui DY. (2002) Low density lipoprotein receptor-related protein mediates apolipoprotein E inhibition of smooth muscle cell migration. *J Biol Chem.* 277(6):4141-6.
27. Haas SL, et al. (2006) Expression of tissue factor in pancreatic adenocarcinoma is associated with activation of coagulation. *World J Gastroenterol.* 12(30):4843-9.
28. Hobbs JE, et al. (2007) Alternatively spliced human tissue factor promotes tumor growth and angiogenesis in a pancreatic cancer tumor model. *Thromb Res.* 120 Suppl 2:S13-21.
29. Pan X, et al. (2008) Nuclear factor-kappaB p65/relA silencing induces apoptosis and increases gemcitabine effectiveness in a subset of pancreatic cancer cells. *Clin Cancer Res.* 14(24):8143-51.
30. van den Berg YW, Versteeg HH. (2010) Alternatively spliced tissue factor. A crippled protein in coagulation or a key player in non-haemostatic processes? *Hamostaseologie.* 30(3):144-9.
31. Rodriguez LG, Wu X, Guan JL. (2005) Wound-healing assay. *Methods Mol Biol.* 294:23-9.
32. Arderiu G, Peña E, Aledo R, Juan-Babot O, Badimon L. (2011) Tissue factor regulates microvessel formation and stabilization by induction of chemokine (C-C motif) ligand 2 expression. *Arterioscler Thromb Vasc Biol.* 31(11):2607-15.
33. Lee SP, et al. (2006) Integrin-linked kinase, a hypoxia-responsive molecule, controls postnatal vasculogenesis by recruitment of endothelial progenitor cells to ischemic tissue. *Circulation.* 114(2):150-9.
34. Nakashima Y, Raines EW, Plump AS, Breslow JL, Ross R. (1998) Upregulation of VCAM-1 and ICAM-1 at atherosclerosis-prone sites on the endothelium in the ApoE-deficient mouse. *Arterioscler Thromb Vasc Biol.* 18(5):842-51.
35. Reynolds LE, et al. (2002) Enhanced pathological angiogenesis in mice lacking beta3 integrin or beta3 and beta5 integrins. *Nat Med.* 8(1):27-34.
36. Boltzen U, et al. (2012) Alternatively spliced tissue factor and full-length tissue factor protect cardiomyocytes against TNF- α -induced apoptosis. *J Mol Cell Cardiol.* [Epub ahead of print, PMID: 22326437].
37. Tsujimoto H, et al. (2005) Flagellin enhances NK cell proliferation and activation directly and through dendritic cell-NK cell interactions. *J Leukoc Biol.* 78(4):888-97.
38. Mancardi S, et al. (2003) Evidence of CXC, CC and C chemokine production by lymphatic endothelial cells. *Immunology.* 108(4):523-30.
39. Abraham D, et al. (2010) Stromal cell-derived CSF-1 blockade prolongs xenograft survival of CSF-1-negative neuroblastoma. *Int J Cancer.* 126(6):1339-52.
40. Alonso F, Boittin FX, Bény JL, Haefliger JA. (2010) Loss of connexin40 is associated with decreased endothelium-dependent relaxations and eNOS levels in the mouse aorta. *Am J Physiol Heart Circ Physiol.* 299(5):H1365-73.
41. Burtea C, et al. (2008) Molecular imaging of alpha v beta3 integrin expression in atherosclerotic plaques with a mimetic of RGD peptide grafted to Gd-DTPA. *Cardiovasc Res.* 78(1):148-57.

42. Couzin-Frankel C. (2010) Inflammation bares a dark side. *Science*. 330(6011):1621.
43. Rüegg C, Alghisi GC. (2010) Vascular integrins: therapeutic and imaging targets of tumor angiogenesis. *Recent Results Cancer Res*. 180:83-101.
44. Desgrosellier JS, et al. (2009) An integrin alpha(v)beta(3)-c-Src oncogenic unit promotes anchorage-independence and tumor progression. *Nat Med*. 15(10):1163-9.
45. Versteeg HH, et al. (2008) Inhibition of tissue factor signaling suppresses tumor growth. *Blood*. 111(1):190-9.
45. Collier ME, Ettelaie C. (2010) Induction of endothelial cell proliferation by recombinant and microparticle-tissue factor involves beta1-integrin and extracellular signal regulated kinase activation. *Arterioscler Thromb Vasc Biol*. 30(9):1810-7.

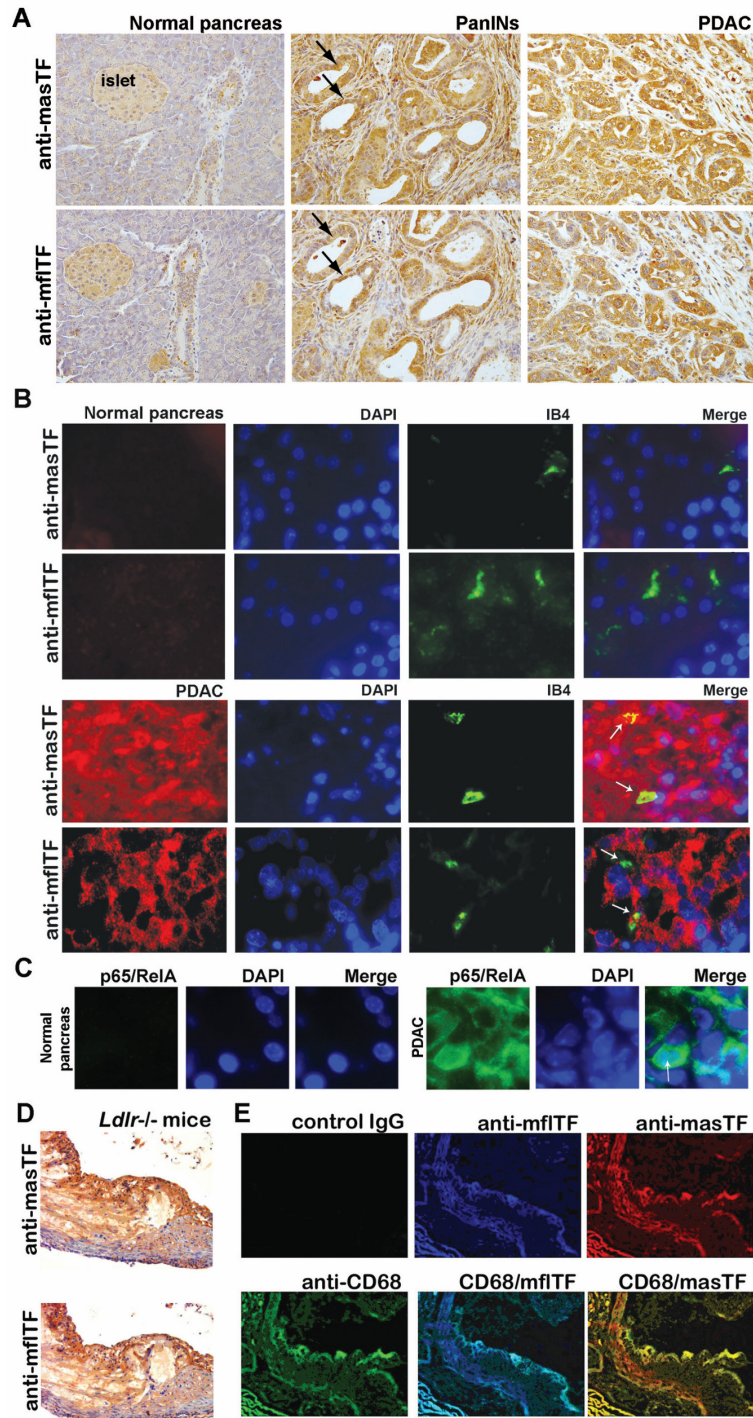


Figure 1. masTF is expressed in pancreatic cancer lesions and aortic plaques. (A,B) Presence and extensive co-localization of masTF and mflTF in serial sections of K-ras induced murine PDAC lesions; white arrows denote microvessels in contact with masTF/mflTF expressing cells and/or masTF-enriched stroma. **(C)** p65/RelA is expressed in PDAC tissue, but not normal pancreas. **(D)** Presence of masTF and mflTF proteins in aortic plaques of *Ldlr*^{-/-} mice; **(E)** masTF co-localizes with mflTF and CD68-positive cells within the plaques.

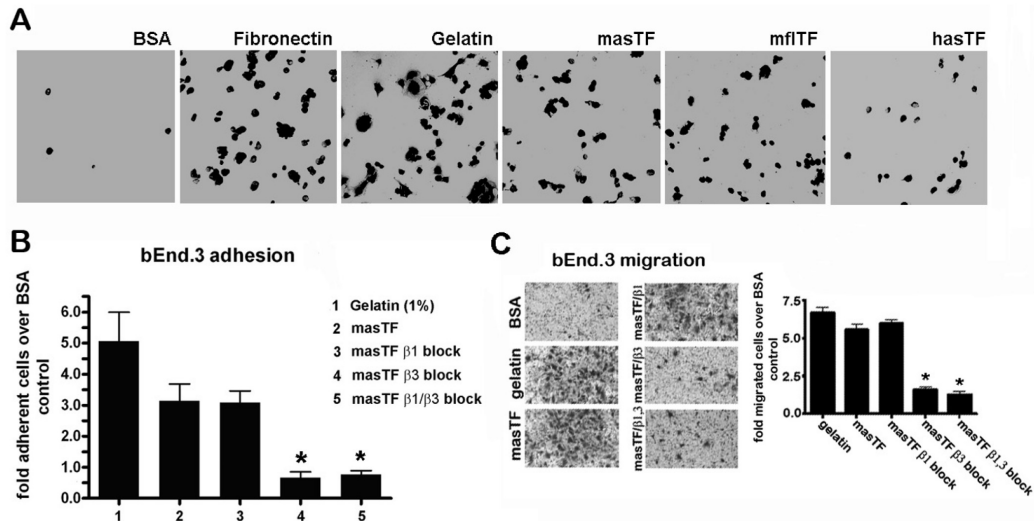


Figure 2. masTF binds β 3 integrins on murine EC and elicits β 3 integrin-dependent cell migration. (A) bEnd.3 cells avidly adhere to masTF, mflTF and hasTF ($n \geq 6$); (B) bEnd.3 cells were pre-incubated with integrin-blocking antibodies and seeded onto BSA- or masTF-coated wells ($n \geq 3$). Flattened cells were counted. (C) Transwell inserts were coated with BSA (negative control), 1% gelatin (positive control), and 50 μ g/mL masTF. Cells were fixed with 4% formaldehyde and stained with 0.1% Crystal Violet; quantifications are shown in the graph, representative images are on the left ($n \geq 3$). * $p < 0.01$.

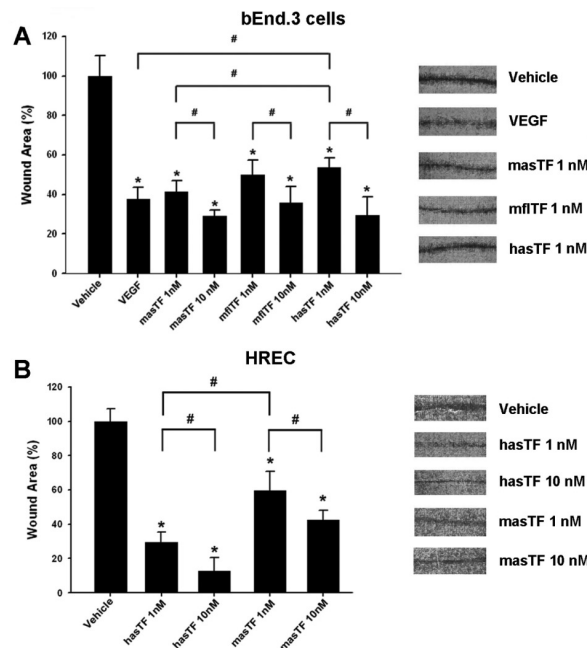


Figure 3. Effects of masTF and hasTF in the scratch assay. bEnd.3 cells (A) and HREC (B) were grown to confluence in six well plates and serum starved overnight in DMEM containing 2% FBS. Eight radial scratches per well were introduced (see Materials and Methods). After 38 hours, cells were washed with PBS, fixed in methanol, and stained with 0.1% Crystal Violet. Representative images of the wounds are on the right ($n \geq 4$). * $p < 0.01$ vs vehicle, # $p < 0.05$.

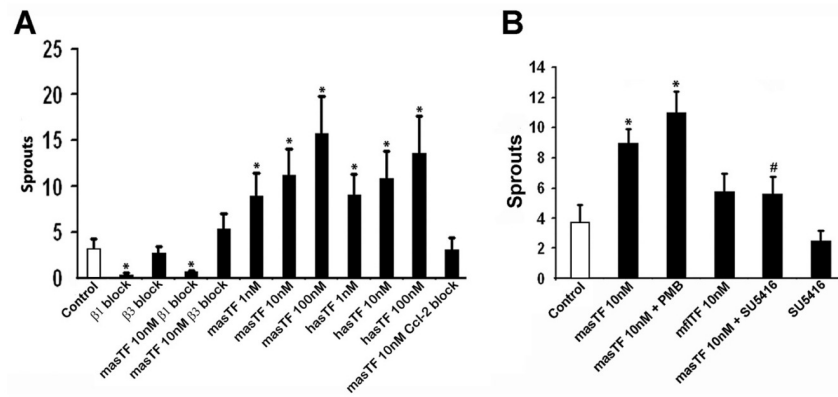


Figure 4. masTF induces aortic sprouting. Murine thoracic aortas were isolated and cleaned of the surrounding tissue in serum-free RPMI containing 100 units/mL penicillin and 100 µg/mL streptomycin. Dissected aortas were flushed with PBS, sectioned into equal segments, embedded in matrigel supplemented with solvent control, masTF, hasTF, or mflTF. Integrin/Ccl2-blocking antibodies (A) or SU5416 (VEGF inhibitor, B) were included in the matrigel when appropriate. PMB, Polymyxin B. Sprouts were counted on day four (n≥4). *p< 0.01 vs control.

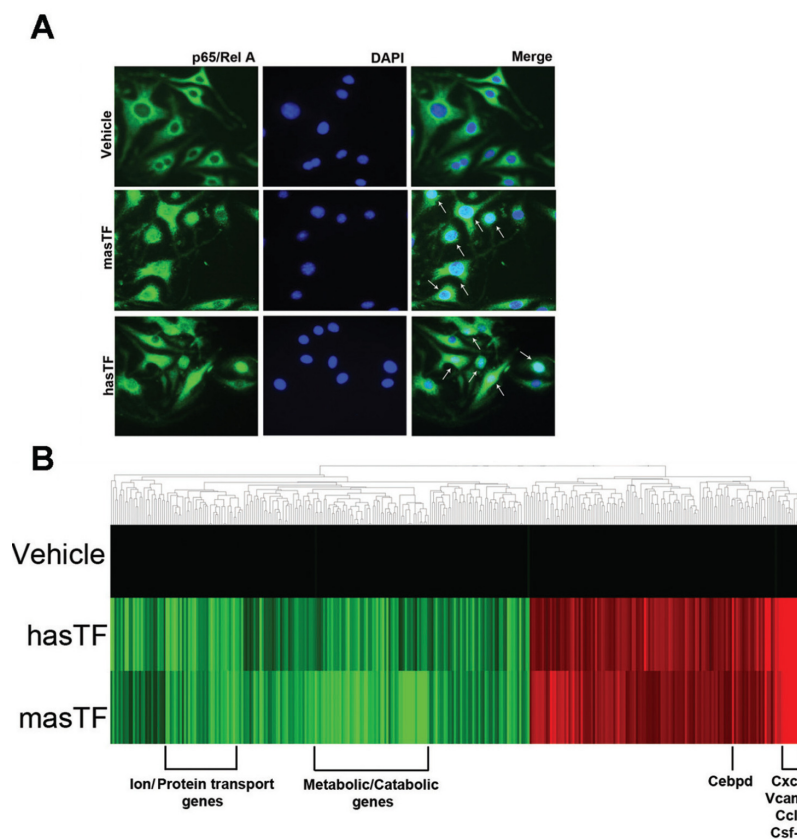


Figure 5. masTF and hasTF elicit analogous changes in the gene expression profile of murine EC. (A) Cellular distribution of p65/Rel A in bEnd.3 cells stimulated with masTF and hasTF (n≥3). White arrows indicate nuclear localization. (B) Heat map, gene cluster analysis of bEnd.3 cells exposed to 50 nM of masTF and 50 nM of hasTF for 4 hrs; 50% glycerol/PBS served as vehicle control. The heat map comprises the genes whose expression were either significantly upregulated by at least 1.2 fold or downregulated by at least 0.9 fold. Results shown are representative of three independent experiments; red denotes upregulation, green denotes downregulation.

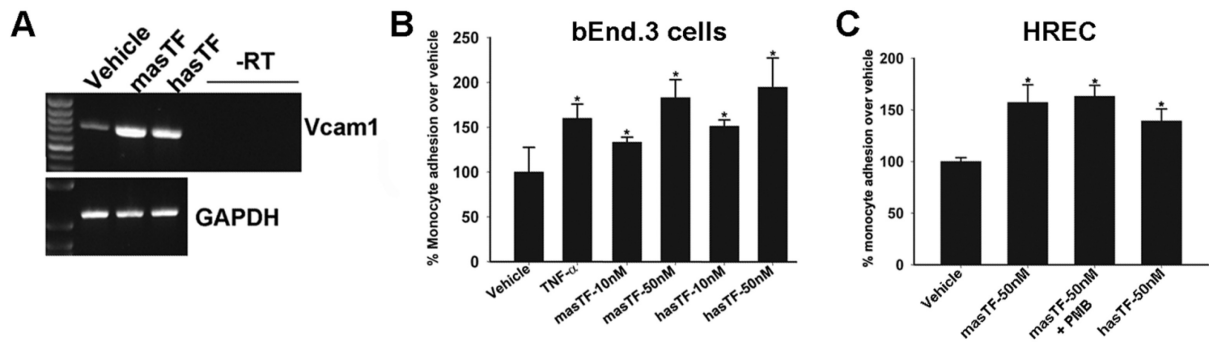
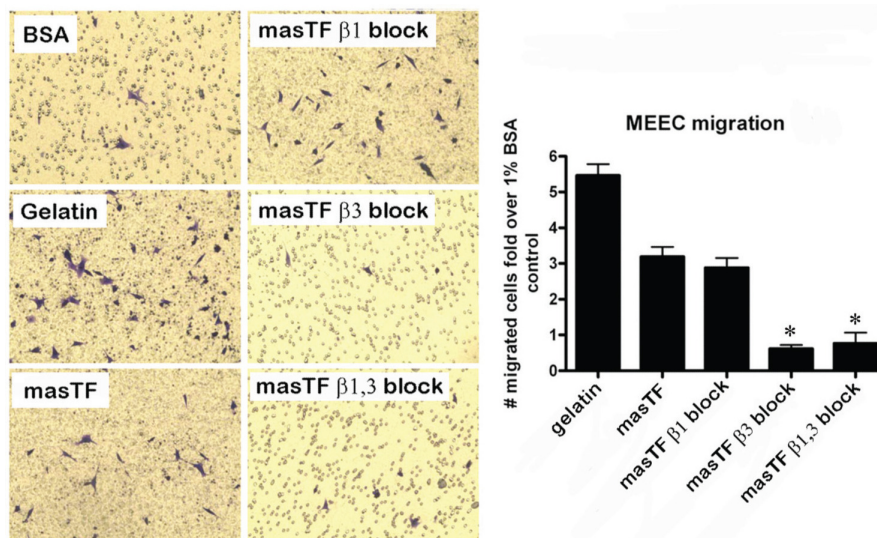


Figure 6. masTF and hasTF promote monocyte adhesion to murine EC. (A) RT-PCR, expression of Vcam-1 in masTF/hasTF stimulated bEnd.3 cells. (B,C) Representative experiment (n=3), orbital shear assay performed using bEnd.3 cells (B) or HREC (C) and pre-labeled J7741.A cells. PMB, Polymyxin B. *p<0.01.



Supplementary Figure 1 masTF elicits β 3 integrin-dependent migration of MEEC. Transwell inserts were coated with BSA (negative control), 1% gelatin (positive control), and 50 μ g/mL masTF, following which MEEC were pre-incubated with integrin-blocking antibodies and seeded onto the wells (n \geq 3). Flattened cells were counted. Cells were fixed with 4% formaldehyde and stained with 0.1% Crystal Violet; quantifications are shown in the graph, representative images are on the left (n \geq 3). *p<0.01 vs masTF.

Supplementary table 1 is available on-line at <http://molmed.org/journal/articles/27/1502>

